Characterizing Quantum Dynamics with Initial System-Environment Correlations

M. Ringbauer,[1,2,*] C. J. Wood,[3,4] K. Modi,[5] A. Gilchrist,[6] A. G. White,[1,2] and A. Fedrizzi[1,2]

[1]*Centre for Engineered Quantum Systems, School of Mathematics and Physics, The University of Queensland, Brisbane, Queensland 4072, Australia*
[2]*Centre for Quantum Computer and Communication Technology, School of Mathematics and Physics, The University of Queensland, Brisbane, Queensland 4072, Australia*
[3]*Institute for Quantum Computing, University of Waterloo, Ontario N2L 3G1, Canada*
[4]*Department of Physics and Astronomy, University of Waterloo, Ontario N2L 3G1, Canada*
[5]*School of Physics, Monash University, Victoria 3800, Australia*
[6]*Centre for Engineered Quantum Systems, Department of Physics and Astronomy, Macquarie University, Sydney, New South Wales 2113, Australia*
(Received 10 October 2014; published 4 March 2015)

We fully characterize the reduced dynamics of an open quantum system initially correlated with its environment. Using a photonic qubit coupled to a simulated environment, we tomographically reconstruct a superchannel—a generalized channel that treats preparation procedures as inputs—from measurement of the system alone. We introduce novel quantitative measures for determining the strength of initial correlations, and to allow an experiment to be optimized in regard to its environment.

In real-world experiments, quantum systems are inevitably coupled to an environment, which usually acts as a source of noise, but it may also be harnessed as a resource—for example in initializing quantum states that may otherwise be unobtainable [1–9]. In either case, understanding the joint behavior of system and environment is essential. Quantum mechanics postulates that the joint system-environment (SE) state evolves unitarily, which need not be true for the system alone. The theory of open quantum systems nevertheless allows for an operationally complete description of the reduced dynamics of the system in cases where the initial SE state is uncorrelated [10]; see Fig. 1(a). This central assumption is often, however, at best an approximation [11,12].

A typical quantum experiment can be split into three steps: state preparation, evolution, and measurement. State preparation takes a system from a generally unknown initial state to a desired input state. This state is then subjected to some dynamical process for a fixed time—the state evolution—and, finally, measured. If the initial system state is correlated with the environment, the system preparation also affects the environment. Consider the extreme case of a maximally entangled initial SE state: $(1/\sqrt{2})(|00\rangle + |11\rangle)_{\mathrm{SE}}$. A projective preparation of the system into $|0\rangle$ or $|1\rangle$ leaves the environment in orthogonal states. Hence, if the subsequent system evolution is not perfectly isolated, it is coupled to different environment states leading to drastically different reduced dynamics of the system conditional on the used preparation procedure [13]. Standard characterization techniques may, in this case, return a description of the reduced system dynamics that appears unphysical [12,14–17]. This highlights the importance of accounting for initial SE correlations to reliably characterize the system dynamics.

While the environment is typically inaccessible to the experimenter, recent results suggest that at least partial information about the initial joint SE state can be extracted from measurements of the system alone. Initial correlations can be witnessed through the distinguishability [18–21] and purity [22] of quantum states, which has also been explored experimentally [23–25]. A more operationally complete characterization can be obtained by explicitly treating the system's preparation procedure, rather than the prepared state, as the input to the reduced description [17].

This *superchannel* approach captures not just the system evolution, but also the dynamical influence of the environment, even in the presence of initial SE correlations. Here we demonstrate this technique experimentally by characterizing the dynamics of a photonic qubit that is
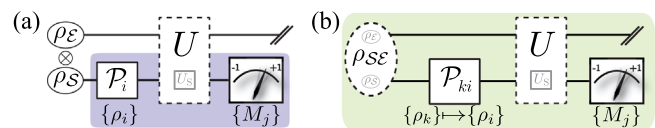

FIG. 1 (color online). System dynamics in the presence of an environment. (a) With no initial SE correlations, the reduced dynamics of the system, which interacts unitarily (U) with an environment, can be completely reconstructed from tomographically complete sets of input states $\{\rho_i\}$ (resulting from preparation procedures $\{\mathcal{P}_i\}$) and measurements $\{M_j\}$. (b) The joint SE state may be initially correlated before the state preparation procedure. The superchannel approach encompasses this situation by treating the preparation procedure P_{ki} as the input state to a more general description of the reduced system dynamics.

initially correlated with a simulated single-photon environment. We introduce novel quantitative measures for the strength of initial SE correlations and for optimizing experiments coupled to an environment.

The state of a d-dimensional open quantum system is described by a density matrix ρ, a positive semidefinite operator with trace one from the set of square matrices $L(\mathcal{X})$, acting on the Hilbert space $\mathcal{X} \cong \mathbb{C}^d$. The evolution of open quantum systems is most generally described by a *channel* $\mathcal{E}: L(\mathcal{X}_1) \to L(\mathcal{X}_2)$, a completely positive (CP) linear map from operators on $L(\mathcal{X}_1)$ to operators on $L(\mathcal{X}_2)$. In the following we assume that $\mathcal{X}_1 = \mathcal{X}_2$ and keep the subscripts to distinguish between input and output Hilbert spaces, though all results apply equally when the input and output spaces are of different dimensions.

A map $\mathcal{E}$ is positive if it preserves an operator's positivity and CP if the same is true for the composite map $\mathcal{I} \otimes \mathcal{E}$, where $\mathcal{I}$ is the identity map on a space at least as large as $\mathcal{X}_1$. Any CP-map $\mathcal{E}$ is completely characterized by its Choi matrix $\Lambda_{\mathcal{E}}$, a positive-semidefinite operator $\Lambda_{\mathcal{E}} \in L(\mathcal{X}_1 \otimes \mathcal{X}_2)$ [26]. The Choi matrix may be constructed via the Choi-Jamiołkowski isomorphism [27] via $\Lambda_{\mathcal{E}} = \sum_{ij} |i\rangle\langle j| \otimes \mathcal{E}(|i\rangle\langle j|)$, where $\{|i\rangle\}_{i=0}^{d-1}$ is an orthonormal basis for $\mathcal{X}_1$, and the evolution of the system state ρ is given by $\mathcal{E}(\rho) = \mathrm{Tr}_{\mathcal{X}_1}[(\rho^T \otimes \mathbb{1})\Lambda_{\mathcal{E}}]$. The Choi matrix of an unknown quantum process can be reconstructed through quantum process tomography (QPT) from the outcomes of a finite set of measurements $\{M_j\}_{j=1}^{d^2}$, performed on a finite set of system input states $\{\rho_i\}_{i=1}^{d^2}$; see Fig. 1(a). Crucially, this assumes that the channel $\mathcal{E}$ being characterized is independent of the system's preparation.

In the presence of initial SE correlations, this assumption is, in general, not satisfied. The joint SE state is then $\rho_{\mathrm{SE}} \in L(\mathcal{X} \otimes \mathcal{Y})$, as illustrated in Fig. 1(b), where $\mathcal{X}$ and $\mathcal{Y}$ are the state spaces of the system and environment, respectively. In the first step of the experiment, the system is prepared in the state ρ_{S} by applying a preparation map $\mathcal{P}$ to S alone. Such a preparation will typically leave the environment in a state conditional on $\mathcal{P}$, which in turn leads to a conditional evolution $\mathcal{E}_{\mathcal{P}}$, and QPT would return a map which is a combination of the partial reconstructions of the possible $\mathcal{E}_{\mathcal{P}}$. In the following, we consider the case of a fully decorrelating preparation procedure: $(\mathcal{P} \otimes \mathcal{I})(\rho_{\mathrm{SE}}) = \rho_{\mathrm{S}} \otimes \rho_{E|\mathcal{P}}$, where $\mathcal{I}$ is the identity map on E. Denoting by $\mathcal{U}$ the channel that describes the subsequent joint evolution, the final output state is given by $\rho_{\mathrm{S}}' = \mathrm{Tr}_E\{\mathcal{U}[(\mathcal{P} \otimes \mathcal{I})(\rho_{\mathrm{SE}})]\}$.

To characterize the system in the presence of possible initial correlations, we describe the dynamics by means of a superchannel $\mathcal{M}: \mathcal{P} \to \rho_{\mathrm{S}}'$. While the CP map $\mathcal{M}$ may be thought of as a regular channel with the input Hilbert space $L(\mathcal{X} \otimes \mathcal{X})$ rather than $L(\mathcal{X})$, we prefer using the term superchannel to emphasize the fact that it takes the preparation channel as an input, rather than the prepared

state. The output is given by $\rho_{\mathrm{S}}' = \mathcal{M}(\Lambda_{\mathcal{P}})$, where $\Lambda_{\mathcal{P}}$ is the Choi matrix for the preparation map $\mathcal{P}$ [17].

We now demonstrate this method by characterizing the superchannel for the evolution of a single photonic qubit. Imagine that the experimenter aims to implement the target system evolution described by the unitary operator U_{S}, chosen as either a Pauli-Z gate ($U_{\mathrm{S}} = Z$), a Hadamard gate ($U_{\mathrm{S}} = H = R_Y Z R_Y^\dagger$), or a rotation ($U_{\mathrm{S}} = Z R_Y$), where R_Y denotes a $\pi/4$ rotation around σ_y. Because of coupling to the environment, the reduced dynamics of the system will, in general, deviate from that described by U_{S}. We simulate this influence by replacing the Z operations in the above decomposition of U_{S} by controlled Z (CZ) operations, switched on and off conditional on the state of the environment, which is modeled as another photonic qubit [28]. In the case of Z and H, the environment might thus cause a failure of the system unitary (i.e., the identity operation is implemented), while in the case $U_{\mathrm{S}} = Z R_Y$ it can introduce a phase error.

The initial SE state was generated via spontaneous parametric down-conversion in the form

$$|\psi\rangle_{\mathrm{SE}} = \cos(2\theta)|H\rangle_{\mathrm{S}}|V\rangle_{\mathrm{E}} + \sin(2\theta)|V\rangle_{\mathrm{S}}|H\rangle_{\mathrm{E}}, \quad (1)$$

where $|H\rangle$, $|V\rangle$ correspond to horizontally and vertically polarized photons, respectively, see Fig. 2. In this case, the strength of the initial correlations (both quantum and classical) is parametrized by the tangle $\tau = \sin^2(4\theta)$ and can be tuned from uncorrelated ($\theta = 0$) to maximal correlation ($\theta = \pi/8$) [32]. We prepared states with $\tau = \{0.012, 0.136, 0.423, 0.757, 0.908\}$, with an average fidelity of $F = 0.96(1)$, with the corresponding ideal state. The system was then subjected to the preparation procedure P_{ij}, which prepared it in the state ρ_j by first projecting onto the state ρ_i, followed by a unitary rotation. Here the indices $i, j \in \{|H\rangle, |V\rangle, |D\rangle, |A\rangle, |R\rangle, |L\rangle\}$, where $|D/A\rangle = (|H\rangle \pm |V\rangle)/\sqrt{2}$ and $|R/L\rangle = (|H\rangle \pm i|V\rangle)/\sqrt{2}$.

From measurements of the system in $\{H, V, D, A, R, L\}$, the operator $\mathcal{M}$ can be directly reconstructed via linear inversion [17]. To avoid known problems with this technique, we instead used maximum likelihood estimation to enforce the reconstruction to be CP; see Supplemental Material [33]. The reconstructed Choi matrix $\Lambda_{\mathcal{M}}$ for $U_{\mathrm{S}} = H$ is illustrated in Fig. 3(a) and the maps for all other target unitaries U_{S} are shown in Ref. [33]. An important property of the superchannel $\mathcal{M}$ is that, in the case of vanishing initial correlations, it factorizes into the density matrix of the effective initial state and the Choi matrix of the effective system channel, $\Lambda_{\mathcal{M}} = \rho_{\mathrm{S}} \otimes \Lambda_{\mathcal{E}}$ [17]. Hence, to allow for an operational interpretation of $\Lambda_{\mathcal{M}}$, we write it using the polarization basis for the index corresponding to the effective initial state, and the Pauli basis for the indices corresponding to the effective channel. Figure 3(b) shows QPT results for the case $U_{\mathrm{S}} = H$, demonstrating how different choices of system preparation procedure can lead
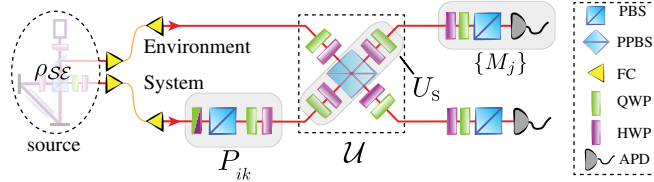
FIG. 2 (color online). Experimental setup. System and environment photons are created in the state ρ_{SE} with controllable degree of entanglement, using the source of Ref. [32]. Arbitrary preparations $\mathcal{P}_{ij}$ on the system and measurements $\{M_j\}$ are implemented by means of polarizers (PBS), quarter- and half-wave plates (QWP, HWP), and single-photon detectors (APD). The joint SE evolution $\mathcal{U}$ is implemented as a CZ gate between a set of HWPs and QWPs. In a case with no initial correlations, this setup implements the target system evolution U_S. The CZ gate is based on nonclassical interference at a partially polarizing beam splitter (PPBS) with reflectivities of $r_H = 0$ ($r_V = 2/3$) for horizontally (vertically) polarized light [40].
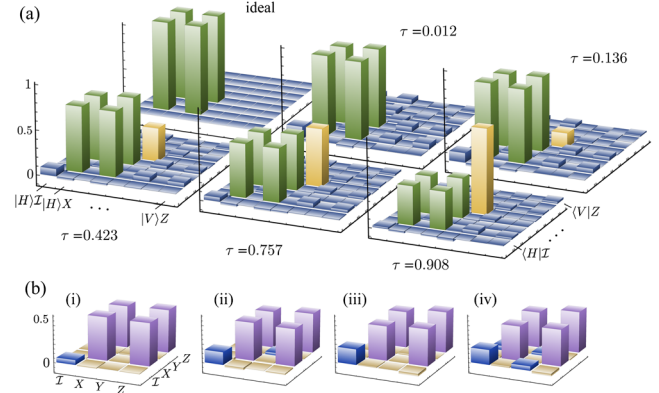

FIG. 3 (color online). (a) Real parts of $\Lambda_{\mathcal{M}}$ for $U_S = H$ in the ideal, uncorrelated case and experimental results for increasingly strong initial correlations. The matrices $\Lambda_{\mathcal{M}}$ are shown in a polarization-Pauli basis, with the elements from left to right corresponding to $\{|H\rangle, |V\rangle\} \otimes \{\mathcal{I}, X, Y, Z\}$ and from front to back corresponding to $\{\langle H|, \langle V|\} \otimes \{\mathcal{I}, X, Y, Z\}$. The emergence of a peak corresponding to the identity operation (shown in yellow) is characteristic for the simulated increased tendency of the single-qubit operation U_S (shown in green) to fail in the presence of stronger initial correlations. The negligible imaginary parts are not shown. (b) Real parts of the Choi matrices (shown in the Pauli basis) for U_S obtained via QPT for different choices of preparation procedure in the case of low initial correlation $\tau = 0.136$. Cases (i) and (ii) correspond to a fixed ρ_k in Fig. 1(b), (iii) corresponds to $\rho_k = \rho_i$, and (iv) is the case where $1 \leq k \leq 4$. The information contained in the superchannel $\mathcal{M}$ can be used to identify the optimal preparation procedure.

to vastly different reconstructed channels, with fidelities varying between 0.853 and 0.683. The superchannel $\mathcal{M}$ in Fig. 3(a) clearly illustrates the reason for this discrepancy: a term that corresponds to the identity operation and increases with the strength of the initial correlations. This is exactly the simulated environment-induced failure mode of the system evolution.

The quantum superchannel $\mathcal{M}$ contains information about initial SE correlations that are visible through their effect on the subsequent experiment, and how different preparation procedures may influence the resulting system dynamics. We now introduce two quantitative measures to extract this information. For any $\mathcal{M}$ we define an *average initial system state* $\rho_{S,\text{av}} = \text{Tr}_{23}[\Lambda_{\mathcal{M}}]/d$ and an *average effective map* for the evolution of the system as $\Lambda_{\mathcal{E}_{\text{av}}} = \text{Tr}_1[\Lambda_{\mathcal{M}}]$. Recall that, for a product initial state ($\rho_{SE} = \rho_S \otimes \rho_E$), the map $\mathcal{M}$ takes the product form $\Lambda_{\mathcal{M}} = \rho_S \otimes \Lambda_{\mathcal{E}}$. In this case $\rho_{S,\text{av}} = \rho_S$, and $\Lambda_{\mathcal{E}_{\text{av}}} = \Lambda_{\mathcal{E}}$ is the Choi matrix of the channel $\mathcal{E}$ describing the (noisy) evolution of the system alone—the same as would result from conventional QPT. For a given $\mathcal{M}$, we can now define the corresponding separable superchannel $\mathcal{M}_s$ via $\Lambda_{\mathcal{M}_s} = (\rho_{S,\text{av}} \otimes \Lambda_{\mathcal{E}_{\text{av}}})$. In general, $\mathcal{M} \neq \mathcal{M}_s$ and the distance between $\mathcal{M}$ and $\mathcal{M}_s$ can be used to quantify the strength of the initial SE correlations. We thus define the *initial correlation (IC) norm* as

$$\|\mathcal{M}\|_{\text{IC}} = \frac{1}{2}\|\mathcal{M} - \mathcal{M}_s\|_{\diamond}. \qquad (2)$$

The matrix $\mathcal{M} - \mathcal{M}_s$ was introduced as the *correlation memory matrix* in Ref. [17] since it describes how the dynamics is affected by initial correlations. Our choice of the diamond norm $\|\cdot\|_{\diamond}$ [41] allows for an operational interpretation of the IC norm in terms of channel discrimination [42]. For any two quantum channels $\mathcal{E}_1, \mathcal{E}_2$, the best

single shot strategy for deciding if a given channel is $\mathcal{E}_1$ or $\mathcal{E}_2$ succeeds with probability $\frac{1}{2}(1 + \frac{1}{2}\|\mathcal{E}_1 - \mathcal{E}_2\|_{\diamond})$. Thus when $\|\mathcal{M}\|_{\text{IC}} = 0$, there is no operational difference between $\mathcal{M}$ and $\mathcal{M}_s$, which means that there are no observable SE correlations. This can either mean that the initial SE state is indeed uncorrelated or that the environment is Markovian and initial correlations do not affect the subsequent dynamics. The initial correlation norm thus provides a necessary and sufficient condition for the decoupling of the future state of the system from its past interactions with the environment. When $\|\mathcal{M}\|_{\text{IC}} > 0$, there exists an optimal preparation procedure that can be used as a witness for initial correlations, and the specific value of the norm determines the single shot probability of success for this witness.

Our measurements of $\|\mathcal{M}\|_{\text{IC}}$, plotted against the correlation strength τ of the simulated initial SE states, are shown in Fig. 4. For all three SE interactions $\mathcal{U}$, the maximum obtained value of $\|\mathcal{M}\|_{\text{IC}}$ is approximately 0.5, which is in agreement with theoretical expectations since, for a maximally correlated initial state, the simulated SE coupling would cause a failure of the evolution with probability 1/2.

The information contained in $\mathcal{M}$ can be further used to optimize the impact of the environment. We introduce the
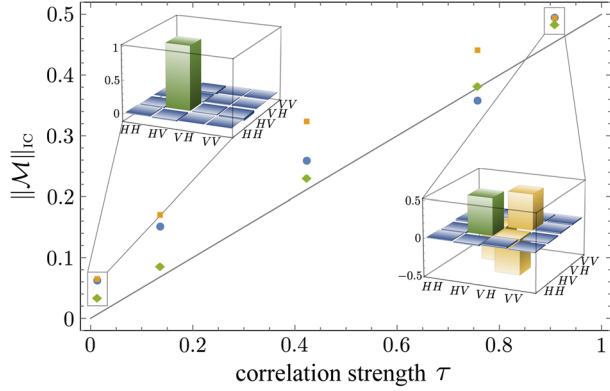
FIG. 4 (color online). Initial correlation norm $\|\mathcal{M}\|_{\mathrm{IC}}$ vs correlation strength τ of ρ_{SE} for $U_{\mathrm{S}} = Z$ (blue circles), $U_{\mathrm{S}} = H$ (yellow squares), and $U_{\mathrm{S}} = ZR_{\mathrm{Y}}$ (green diamonds). The values of τ were obtained from state tomography of ρ_{SE} for each experiment. The measured real parts of the states with weakest and strongest initial correlations are shown in the respective insets. The solid line corresponds to the IC norm in the ideal case. Error bars from Poissonian counting statistics are on the order of the symbol size.

measure of *preparation fidelity* F_{prep} for the case where high-fidelity projective preparation procedures are readily available, such as in photonic experiments, noting that similar measures could be defined for other scenarios. Consider a system preparation via initial postselection on the state ρ_1. The subsequent evolution is then described by the effective map $\mathcal{E}_{\rho_1}$ given by

$$\Lambda_{\mathcal{E}_{\rho_1}} = \frac{1}{p_{\rho_1}} \mathrm{Tr}_1 [(\rho_1^\dagger \otimes \mathbb{1}_{23}) \Lambda_{\mathcal{M}}], \qquad (3)$$

where $p_{\rho_1} = \mathrm{Tr}[(\rho_1^\dagger \otimes \mathbb{1}_{23}) \Lambda_{\mathcal{M}}]/d$ is the probability of success for the postselection on ρ_1. Studying these effective maps for different states ρ_1 allows us to find the optimal preparation procedure for any desired evolution of the system. The measure F_{prep} quantifies the process fidelity between the implemented effective map $\mathcal{E}_{\rho_1}$ and the desired target channel U_{S} for initial projection onto ρ_1,

$$F_{\mathrm{prep}}(\mathcal{M}, \rho_1, U_{\mathrm{S}}) = \frac{1}{d^2} F(\Lambda_{\mathcal{E}_{\rho_1}}, \Lambda_{U_{\mathrm{S}}}). \qquad (4)$$

The average preparation fidelity over all initial projections can be obtained from $\Lambda_{\overline{\mathcal{E}_{\rho_1}}} = \Lambda_{\mathcal{E}_{\mathrm{av}}} = \mathrm{Tr}_1[\Lambda_{\mathcal{M}}]$. Maximizing F_{prep} over all states ρ_1 for a given target unitary U_{S} finds a preparation which allows for the highest quality implementation of U_{S}. Note that this is not equivalent to minimizing the impact of the environment since the optimal preparation might harness some of the environmental correlations to improve the gate performance.

We now use our experimentally obtained $\mathcal{M}$ to optimize for maximum fidelity for the target $U_{\mathrm{S}} = Z$, Fig. 5(a), and $U_{\mathrm{S}} = ZR_{\mathrm{Y}}$, Fig. 5(b), given a correlation strength of
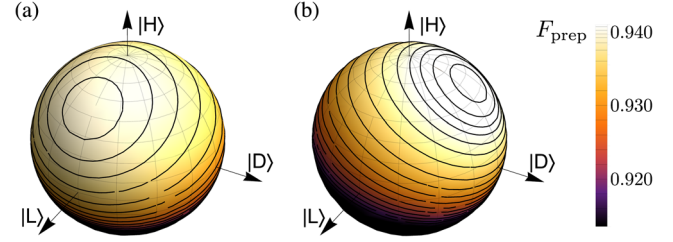

FIG. 5 (color online). Optimization of the preparation procedure. The average preparation fidelity $F_{\mathrm{prep}}(\mathcal{M}, \rho_1, Z)$ for (a) $U_{\mathrm{S}} = Z$ and (b) $U_{\mathrm{S}} = ZR_{\mathrm{Y}}$ is shown as a density plot on the surface of the Bloch sphere of the initial-projection state ρ_1. In both cases, we chose the lowest strength of initial correlation realized in the experiment to visualize the effect even for very weak SE correlations.

$\|\mathcal{M}\|_{\mathrm{IC}} = 0.062(5)$ and $\|\mathcal{M}\|_{\mathrm{IC}} = 0.034(2)$, respectively. In Fig. 5(a), the effect of the environment is minimized for initial projection onto the state $\cos[\phi]|H\rangle + e^{i\varphi} \sin[\phi]|V\rangle$ with $\phi \approx 0.658$ and $\varphi \approx 0.252$. This demonstrates that, even for nearly uncorrelated SE states, the chosen preparation procedure affects the achieved fidelity. In this example, the projection on the optimal state instead of the basis state $|H\rangle$ improved the fidelity by 0.2%. Similarly, minimizing F_{prep} finds the worst-case preparation, which could give insight into where and why an experimental setup fails.

We demonstrated here that the superchannel approach to characterizing system dynamics coupled to an environment is—in contrast to some previous work on open system dynamics—operationally significant and experimentally accessible. This approach applies to the most general case, where the conditions that lead to CP reduced-dynamics [43–46] might not be met. Notably, the reconstruction of $\mathcal{M}$ is a direct generalization of QPT, based on subjecting the system to d^4, rather than d^2 linearly independent preparation procedures $\mathcal{P}_{ij}$, which need not all be fully decorrelating. Therefore, tools developed to improve the efficiency of QPT, such as compressive sensing [47,48] can also be applied to the reconstruction of $\mathcal{M}$.

Since the output of a channel is determined solely by the input and the channel itself, it can be thought of as a Markovian two-point connection. The presence of initial correlations, however, demands the use of the superchannel approach, which is thus an important step towards understanding non-Markovian quantum processes. Along these lines, the superchannel approach has recently been used to derive the lower bound on entropy production in a generic quantum process [49].

Our technique is most useful in quantum architectures which are strongly coupled to their environment, such as spins in local spin baths. Another application is in quantum control, where control time scales can be much faster than environmental reset times. Finally, it has been suggested that non-Markovianity can be exploited as a resource [50];

---

*Corresponding author.
m.ringbauer@uq.edu.au

[1] M. B. Plenio, S. F. Huelga, A. Beige, and P. L. Knight, Phys. Rev. A **59**, 2468 (1999).

[2] S. Bose, P. L. Knight, M. B. Plenio, and V. Vedral, Phys. Rev. Lett. **83**, 5158 (1999).

[3] A. Beige, D. Braun, B. Tregenna, and P. L. Knight, Phys. Rev. Lett. **85**, 1762 (2000).

[4] S. Diehl, A. Micheli, A. Kantian, B. Kraus, H. P. Büchler, and P. Zoller, Nat. Phys. **4**, 878 (2008).

[5] J. T. Barreiro, M. Müller, P. Schindler, D. Nigg, T. Monz, M. Chwalla, M. Hennrich, C. F. Roos, P. Zoller, and R. Blatt, Nature (London) **470**, 486 (2011).

[6] C. Cormick, A. Bermudez, S. F. Huelga, and M. B. Plenio, New J. Phys. **15**, 073027 (2013).

[7] Y. Lin, J. P. Gaebler, F. Reiter, T. R. Tan, R. Bowler, A. S. Sørensen, D. Leibfried, and D. J. Wineland, Nature (London) **504**, 415 (2013).

[8] J.-S. Xu, K. Sun, C.-F. Li, X.-Y. Xu, G.-C. Guo, E. Andersson, R. Lo Franco, and G. Compagno, Nat. Commun. **4**, 2851 (2013).

[9] C. J. Wood, T. W. Borneman, and D. G. Cory, Phys. Rev. Lett. **112**, 050501 (2014).

[10] F. Petruccione and H.-P. Breuer, *The Theory of Open Quantum Systems* (Oxford University Press, New York, 2002).

[11] C. A. Rodríguez-Rosario, K. Modi, A.-M. Kuah, A. Shaji, and E. C. G. Sudarshan, J. Phys. A **41**, 205301 (2008).

[12] K. Modi and E. C. G. Sudarshan, Phys. Rev. A **81**, 052119 (2010).

[13] K. Modi, Open Syst. Inf. Dyn. **18**, 253 (2011).

[14] A.-M. Kuah, K. Modi, C. A. Rodríguez-Rosario, and E. C. G. Sudarshan, Phys. Rev. A **76**, 042113 (2007).

[15] M. Ziman, arXiv:quant-ph/0603166.

[16] H. A. Carteret, D. R. Terno, and K. Zyczkowski, Phys. Rev. A **77**, 042113 (2008).

[17] K. Modi, Sci. Rep. **2**, 581 (2012).

[18] S. Wißmann, B. Leggio, and H.-P. Breuer, Phys. Rev. A **88**, 022108 (2013).

[19] E.-M. Laine, J. Piilo, and H.-P. Breuer, Europhys. Lett. **92**, 60010 (2010).

[20] C. A. Rodríguez-Rosario, K. Modi, L. Mazzola, and A. Aspuru-Guzik, Europhys. Lett. **99**, 20010 (2012).

[21] M. Gessner and H.-P. Breuer, Phys. Rev. Lett. **107**, 180402 (2011).

[22] D. Z. Rossatto, T. Werlang, L. K. Castelano, C. J. Villas-Boas, and F. F. Fanchini, Phys. Rev. A **84**, 042113 (2011).

[23] A. Smirne, D. Brivio, S. Cialdi, B. Vacchini, and M. G. A. Paris, Phys. Rev. A **84**, 032112 (2011).

[24] C.-F. Li, J.-S. Tang, Y.-L. Li, and G.-C. Guo, Phys. Rev. A **83**, 064102 (2011).

[25] M. Gessner, M. Ramm, T. Pruttivarasin, A. Buchleitner, H.-P. Breuer, and H. Häffner, Nat. Phys. **10**, 105 (2013).

[26] M.-D. Choi, Linear Algebra Appl. **10**, 285 (1975).

[27] A. Jamiołkowski, Rep. Math. Phys. **3**, 275 (1972).

[28] This is sufficient to describe a large range of joint SE dynamics, including common error channels, and to illustrate the technique [23,29], although a slightly larger environment would be required in the most general case [30,31].

[29] A. Chiuri, C. Greganti, L. Mazzola, M. Paternostro, and P. Mataloni, Sci. Rep. **2**, 968 (2012).

[30] B. Schumacher, Phys. Rev. A **54**, 2614 (1996).

[31] G. Narang and Arvind, Phys. Rev. A **75**, 032305 (2007).

[32] A. Fedrizzi, T. Herbst, A. Poppe, T. Jennewein, and A. Zeilinger, Opt. Express **15**, 15377 (2007).

[33] See Supplemental Material at http://link.aps.org/supplemental/10.1103/PhysRevLett.114.090402, which includes Refs. [34–39], for details on the reconstruction of $\mathcal{M}$ using linear inversion and maximum likelihood estimation.

[34] Z. Hradil, Phys. Rev. A **55**, R1561 (1997).

[35] D. F. V. James, P. G. Kwiat, W. J. Munro, and A. G. White, Phys. Rev. A **64**, 052312 (2001).

[36] R. Blume-Kohout, New J. Phys. **12**, 043034 (2010).

[37] M. Grant and S. Boyd, computer code CVX, 2014.

[38] R. Blume-Kohout, Phys. Rev. Lett. **105**, 200504 (2010).

[39] C. J. Wood, J. D. Biamonte, and D. G. Cory, Tensor networks and graphical calculus for open quantum systems, arXiv:1111.6950.

[40] N. K. Langford, T. J. Weinhold, R. Prevedel, K. J. Resch, A. Gilchrist, J. L. O'Brien, G. J. Pryde, and A. G. White, Phys. Rev. Lett. **95**, 210504 (2005).

[41] A. Y. Kitaev, Russ. Math. Surv. **52**, 1191 (1997).

[42] B. Rosgen and J. Watrous, in *Proceedings of the 20th Annual IEEE Conference on Computational Complexity, San Jose, CA, 2005* (IEEE, New York, 2005), p. 344.

[43] A. Shabani and D. A. Lidar, Phys. Rev. Lett. **102**, 100402 (2009).

[44] A. Brodutch, A. Datta, K. Modi, A. Rivas, and C. A. Rodríguez-Rosario, Phys. Rev. A **87**, 042301 (2013).

[45] J. M. Dominy, A. Shabani, and D. A. Lidar, A general framework for complete positivity, arXiv:1312.0908.

[46] F. Buscemi, Phys. Rev. Lett. **113**, 140502 (2014).

[47] A. Shabani, R. L. Kosut, M. Mohseni, H. Rabitz, M. A. Broome, M. P. Almeida, A. Fedrizzi, and A. G. White, Phys. Rev. Lett. **106**, 100401 (2011).

[48] S. T. Flammia, D. Gross, Y.-K. Liu, and J. Eisert, New J. Phys. **14**, 095022 (2012).

[49] S. Vinjanampathy and K. Modi, Second law for quantum operations, arXiv:1405.6140.

[50] B. Bylicka, D. Chruscinski, and S. Maniscalco, Sci. Rep. **4**, 5720 (2014).